

# High Stress Abrasive Wear Behavior of Sillimanite-Reinforced Al-Alloy Matrix Composite: A Factorial Design Approach

M. Singh, D.P. Mondal, A.K. Jha, and A.H. Yegneswaran

(Submitted 18 April 2000)

An attempt has been made to explore the possibility of using a natural mineral, namely sillimanite, as dispersoid for synthesizing aluminum alloy composite by solidification technique. The abrasive wear behavior of this composite has been studied through factorial design of experiments. The wear behavior of the composite ( $Y_{\text{composite}}$ ) and the alloy ( $Y_{\text{alloy}}$ ) is expressed in terms of the coded values of different experimental parameters like applied load ( $x_1$ ), abrasive size ( $x_2$ ), and sliding distance ( $x_3$ ) by the following linear regression equations:

$$Y_{\text{alloy}} = 20.94 + 15.22x_1 + 5.94x_2 - 1.95x_3 + 4.82x_1x_2 - 1.48x_1x_3 + 1.29x_2x_3 + 1.60x_1x_2x_3$$

$$Y_{\text{composite}} = 21.05 + 15.69x_1 + 9.5x_2 - 2.51x_3 + 7.41x_1x_2 - 2.33x_1x_3 + 0.52x_2x_3 + 0.10x_1x_2x_3$$

These equations suggest that (i) the effect of the load is more severe on the wear rate of each of the materials and (ii) the wear rate of the materials increases with an increase in applied load and abrasive size, but decreases with increase in sliding distance (iii) interaction of these parameters are quite significant towards the wear of these materials (iv) above a critical load and abrasive size the composite suffers from higher wear rate than that of the matrix alloy. These facts have been explained on the basis of wear mechanisms.

**Keywords** aluminum matrix composite, factorial design, natural mineral, sillimanite particles, two body abrasive wear

## 1. Introduction

Aluminum alloy metal matrix composites are attracting considerable attention for the fabrication of engineering components due to their versatile and tailor made properties.<sup>[1]</sup> These materials can be prepared by using different types of aluminum alloys as matrix material and a variety of materials like silicon carbide,<sup>[2-4]</sup> alumina,<sup>[5-8]</sup> zircon,<sup>[9]</sup> etc., in fiber, whisker, and particulate form as dispersoid depending on property requirements for the application. Some of the natural minerals have lot of potential to be used as dispersoids for making composites.<sup>[10]</sup> Natural minerals like talc,<sup>[11]</sup> bauxite,<sup>[12]</sup> corundum,<sup>[13]</sup> granite,<sup>[14]</sup> etc., have already been used in particulate form to develop aluminum alloy composites for wear-resistant applications. Sillimanite, a natural mineral, possesses adequate thermal stability and mechanical properties. This mineral is available in abundance and is less expensive. Thus, sillimanite could be a promising dispersoid material for synthesizing composites especially for wear-resistant applications. These composite materials may be used as wear-resistant components like brake drum, piston, cylinder heads, and liners in the automobile sector and apex insert and pump bodies in the mineral dressing

industry. This leads to the need for characterizing the wear behavior of composites.

In most of these applications, wear is generally abrasive in nature. Abrasive wear is defined as the displacement of the material caused by hard particles or protuberances where these particles are forced against and moving along a solid surface. It has been reported that the wear behavior of composite depends on microstructural characteristics like shape, size, volume fraction, and distribution of the reinforcement and the experimental parameters like abrasive size, applied load, sliding distance, etc.<sup>[15,16]</sup>

In addition to this, the wear of composite is also dictated by its strength, hardness, and fracture toughness.<sup>[15]</sup> It has been reported that above a critical size of abrasion, the wear rate of the composite becomes invariant to the abrasive size.<sup>[17,18]</sup> It is further reported that the composite may suffer from higher wear rate than the alloy above a critical applied load. This is primarily due to deeper and wider wear grooves generated under certain combinations of applied load and abrasive size. Moore and Douthwaite reported that the surface or subsurface of the specimen undergoes plastic deformation during abrasive wear and the extent of plastically deformed zone depends on applied load and abrasive size.<sup>[19]</sup> However, the severity of the combined effect of applied load and abrasive size on the wear rate has not been studied systematically. The effect of sliding distance on the abrasive wear of Al-alloy composite has been studied by several investigators,<sup>[20]</sup> but the synergic effect of sliding distance, abrasive size, and applied load has not been examined. This paper aims to examine the individual and combined effect of load, abrasive size, and sliding distance on the high-stress abrasive wear behavior of Al-alloy sillimanite par-

M. Singh, D.P. Mondal, A.K. Jha, and A.H. Yegneswaran, Regional Research Laboratory (CSIR), Hoshangabad Road, Near Habibganj Naka, Bhopal-462 026, India. Contact e-mail: mulayam\_singh@hotmail.com.

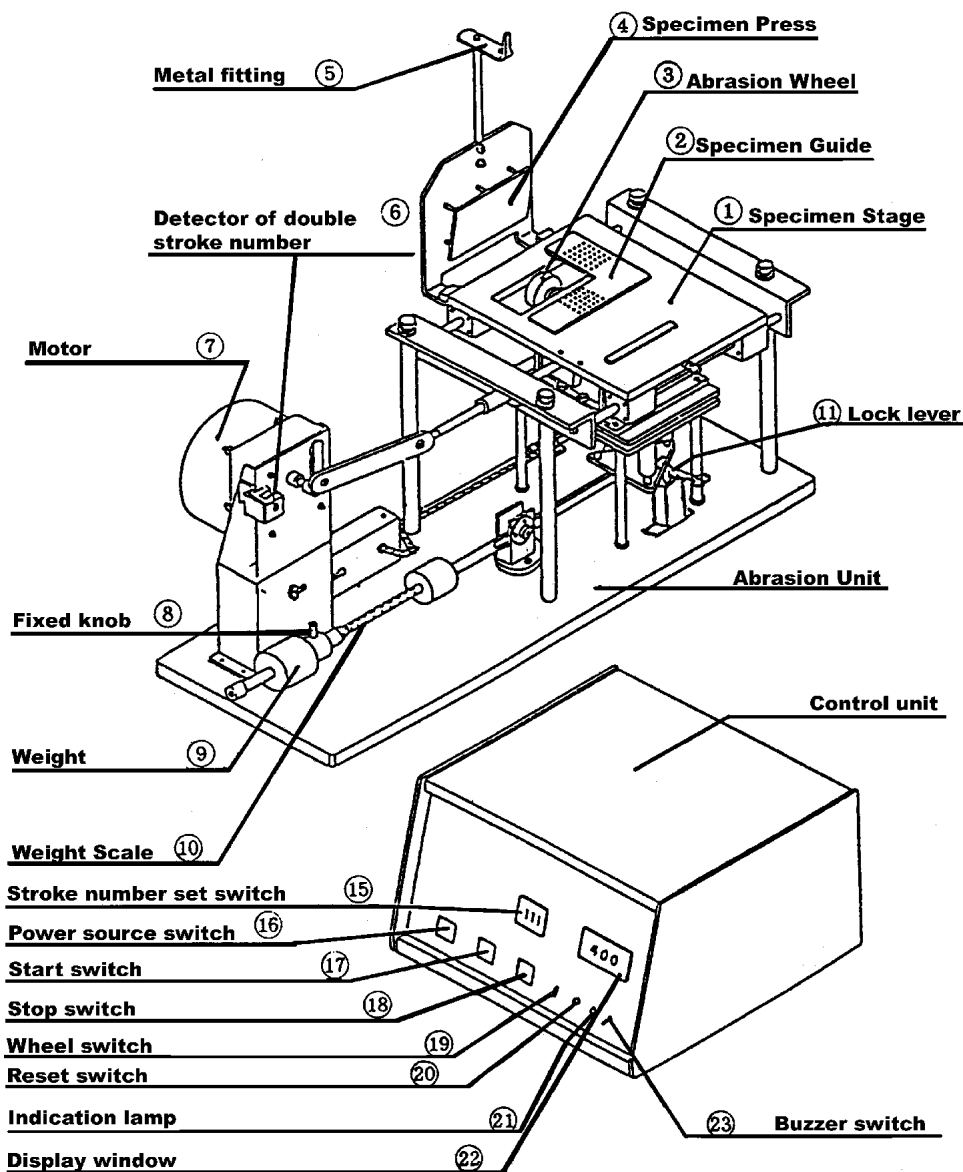


Fig. 1 Schematic diagram of abrasion test machine

ticle composites. This study was carried out using the factorial design approach.

## 2. Experimental

### 2.1 Materials

Aluminum alloy (BS: LM 6) containing (13% Si-0.6% Fe-0.1% Cu-0.1% Mg-0.5% Mn) was used as the matrix alloy. The alloy was melted in a graphite crucible. In the alloy melt, preheated 10 wt.% sillimanite particles (50-150  $\mu\text{m}$ ) were added by creating a vortex in the melt with the help of a stirrer. After thoroughly mixing composite samples were cast in permanent disc moulds (120 mm diameter and 6 mm thick). The matrix alloy was also processed in a similar manner to compare the results.

The cast composite samples  $15 \times 15 \text{ mm}^2$  were metallographically polished and etched in Keller's etchant. The etched samples were sputter coated with a thin layer of gold and the microstructure was examined using scanning electron microscope (SEM) (Jeol, Model JSM 5600, Akishima, Tokyo, Japan).

### 2.2 Abrasion Test

High-stress abrasion tests were carried on  $40 \times 35 \times 4 \text{ mm}^3$  rectangular specimens using a Suga Abrasion Tester (Model: NUS 1, Tokyo, Japan). A schematic view of the abrasion test machine is shown in Fig. 1. Emery paper embedded with the desired size of SiC particles was cut to size and fixed on a wheel (50 mm diameter, 12 mm thick) to serve as the abrasive medium. The specimen was fixed against the abrasive medium, and the load was applied with the help of a cantilever mecha-

nism. The specimen was subjected to a reciprocating motion against the abrasive medium. The abrasive wheel was also rotated slowly to enable the specimen to encounter fresh abrasive particles in each cycle prior to traversing a distance of 26 m. Beyond this sliding distance, the degraded abrasive again came into contact with the specimen surface.

Applied loads in the current study were 1, 3, 5, and 7 N, and the abrasive medium contained 25, 100, and 200  $\mu\text{m}$  SiC particles. Weight loss of the specimen was measured after a sliding distance of 26 m. Wear rate was calculated from the weight loss data.

A Mettler (Switzerland) microbalance was used for weighing the specimens before and after the test. The specimens were cleaned before and after the tests. The composite and matrix alloy specimens were tested under identical test conditions to enable comparison. Worn surfaces of the selected specimens were examined in the SEM to study the wear mechanism. Prior to SEM study, specimens were coated with a thin layer of gold.

### 2.3 Factorial Design of Experiments

A factorial design of experiments of the type  $P^n$  was used in which  $n$  corresponds to number of factors and  $P$  represents the number of levels.<sup>[21]</sup> Here  $n = 3$  (i.e., load, abrasive size, and sliding distance) and  $p = 2$ . Thus the minimum number of trials needed for investigation is  $2^3 = 8$ . If the response variable (i.e., wear rate) is represented by  $Y$ , the linear regression equation for these experiments may be expressed as

$$Y = a_0 + a_1x_1 + a_2x_2 + a_3x_3 + a_4x_1x_2 + a_5x_1x_3 + a_6x_2x_3 + a_7x_1x_2x_3 \quad (\text{Eq 1})$$

where  $a_0$  is the response variable at the base level and  $a_1, a_2, a_3$  are the coefficients representing the severity effects of individual variables like load, abrasive size and sliding distance;  $x_1, x_2,$  and  $x_3$  are the coded values of load, abrasive size, and distance, respectively;  $a_4, a_5,$  and  $a_6$  represent interaction coefficients of variables  $x_1$  and  $x_2, x_1$  and  $x_3, x_2$  and  $x_3,$  respectively; and  $a_7$  represents the interaction coefficient among the variables  $x_1, x_2,$  and  $x_3$  within the selected levels of each variable. This signifies the severity of the synergic effect of these parameters toward wear.

The methodology for calculating the values for each regression coefficient using the coded value of each factor is described elsewhere.<sup>[22]</sup> The positive value of  $Y$  in Eq 1 indicates weight loss while a negative value of same means weight gain. Further, a negative value of any term in equation signifies reduction in the rate of material loss due to increase in the value of the respective parameter. The coded value of each parameter is calculated using following relation:

$$\text{Coded value} = \frac{\text{Selected value} - \text{Base value}}{\text{Difference between base value to upper or lower level}}$$

The upper and lower levels of each factor along with their coded values are shown in Table 1. The factorial design of the experiments and the values of the response variables corresponding to each trial are reported in Table 2. The matrix

**Table 1 Levels of Different Factors and Their Coded Values (Within Brackets)**

| Factor Level and Code | Factors |                     |          |
|-----------------------|---------|---------------------|----------|
|                       | Load    | Abrasive Size       | Distance |
| Upper level           | 7 N     | 200 $\mu\text{m}$   | 130 m    |
| Code value            | (+1)    | (+1)                | (+1)     |
| Base value            | 4 N     | 112.5 $\mu\text{m}$ | 78 m     |
| Code value            | (0)     | (0)                 | (0)      |
| Lower level           | 1 N     | 25 $\mu\text{m}$    | 26 m     |
| Code value            | (-1)    | (-1)                | (-1)     |

**Table 2 Values of Individual Variables With Their Coded Values (Within Brackets) and Wear Response in Each Trial**

| Trial No. | Load, N, $x_1$ | Abrasive Size, $\mu\text{m}, x_3$ | Distance | Wear Rate, $Y \times 10^{-11} \text{ m}^3/\text{m}$ |           |
|-----------|----------------|-----------------------------------|----------|---|-----------|
|           |                |                                   |          | Alloy   | Composite |
| 1         | 7 (+1)         | 200 (+1)                          | 130 (+1) | 45.84   | 49.42     |
| 2         | 7 (+1)         | 200 (+1)                          | 26 (-1)  | 48  | 57.88     |
| 3         | 7 (+1)         | 25 (-1)                           | 26 (-1)  | 31.2  | 25.28     |
| 4         | 1 (-1)         | 200 (+1)                          | 26 (-1)  | 7.08  | 7.21      |
| 5         | 1 (-1)         | 25 (-1)                           | 130 (+1) | 3.9   | 2.68      |
| 6         | 1 (-1)         | 25 (-1)                           | 26 (-1)  | 5.3   | 3.87      |
| 7         | 1 (-1)         | 200 (+1)                          | 130 (+1) | 6.6   | 7.7       |
| 8         | 7 (+1)         | 25 (-1)                           | 130 (+1) | 19.6  | 14.38     |

design for calculating each coefficient of Eq 1 is shown in Table 3.

## 3. Results

### 3.1 Microstructure

Figure 2(a) shows the microstructure of the composite. It clearly reveals reasonably uniform distribution of sillimanite particles in the matrix. A high-magnification micrograph is showing sound interfacial bonding of the sillimanite particles with the alloy matrix (Fig. 2b). It is noted from Fig. 2(b) that the sillimanite particle is primarily surrounded by eutectic silicon. This may be attributed to the fact that the sillimanite particles are pushed by the solidification front to the last freezing liquid (i.e., eutectic).<sup>[23]</sup>

### 3.2 Linear Regression Equations

The final linear regression equations of the matrix alloy and the composite are shown below:

$$Y_{\text{alloy}} = 20.94 + 15.22x_1 + 5.94x_2 - 1.95x_3 + 4.82x_1x_2 - 1.48x_1x_3 + 1.29x_2x_3 + 1.60x_1x_2x_3 \quad (\text{Eq 2})$$

$$Y_{\text{composite}} = 21.05 + 15.69x_1 + 9.5x_2 - 2.51x_3 + 7.41x_1x_2 - 2.33x_1x_3 + 0.52x_2x_3 + 0.10x_1x_2x_3 \quad (\text{Eq 3})$$

where the multiplication factor is  $10^{-11} \text{ m}^3/\text{m}$  and  $x_1, x_2,$  and  $x_3$

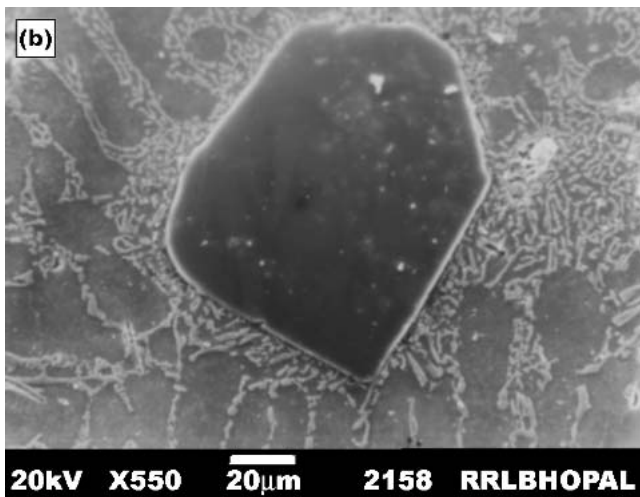
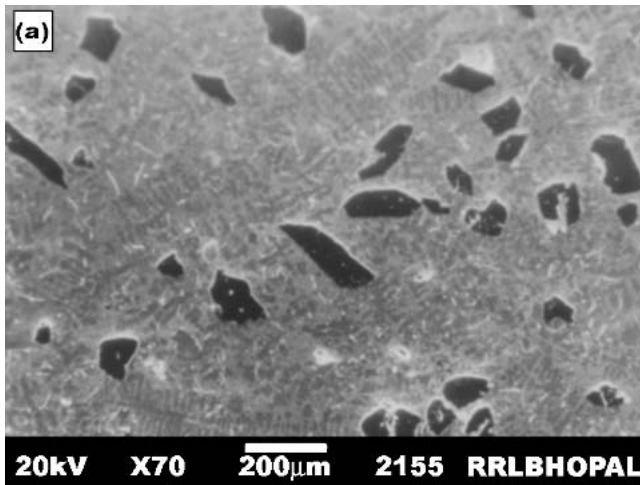


**Fig. 2** (a) Microstructure of the composite showing uniform distribution of sillimanite particles; (b) magnified view of the microstructure showing good particle/matrix interfacial bonding

**Table 3** Matrix Design to Calculate Regression Coefficient

| Exp. No. | $x_1$ | $x_2$ | $x_3$ | $x_1x_2$ | $x_1x_3$ | $x_2x_3$ | $x_1x_2x_3$ | Wear Rate, Alloy | $Y \times 10^{-11}$ m <sup>3</sup> /m, Composite |
|----------|-------|-------|-------|----------|----------|----------|-------------|------------------|--|
| 1        | +1    | +1    | +1    | +1       | +1       | +1       | +1          | 45.84            | 49.42  |
| 2        | +1    | +1    | -1    | +1       | -1       | -1       | -1          | 48               | 57.88  |
| 3        | +1    | -1    | -1    | -1       | -1       | +1       | +1          | 31.2             | 25.28  |
| 4        | -1    | +1    | -1    | -1       | +1       | -1       | +1          | 7.08             | 7.21   |
| 5        | -1    | -1    | +1    | +1       | -1       | -1       | +1          | 3.9              | 2.68   |
| 6        | -1    | -1    | -1    | +1       | +1       | +1       | -1          | 5.3              | 3.87   |
| 7        | -1    | +1    | +1    | -1       | -1       | +1       | -1          | 6.6              | 7.7  |
| 8        | +1    | -1    | +1    | -1       | +1       | -1       | -1          | 19.62            | 14.38  |

are coded values of load, abrasive size, and distance, respectively. By comparing Eq (1), (2), and (3), it is noted that the values of  $a_0$  for the alloy and the composite are 20.94 and 21.05, respectively, and it represents the value of response variable (wear rate) at the base level (load of 4 N, abrasive size

**Table 4** Comparison of Theoretical and Experimental Wear Rates of Different Materials at Abrasive Size of 100  $\mu\text{m}$

| Load, N | Distance, m | Wear Rate $\times 10^{-11}$ m <sup>3</sup> /s |       |             |           |       |             |
|---------|-------------|---|-------|-------------|-----------|-------|-------------|
|         |             | Alloy   |       |             | Composite |       |             |
|         |             | Theo.   | Exp.  | % Deviation | Theo.     | Exp.  | % Deviation |
| 3       | 26          | 16.895  | 18.25 | 7.4         | 16.67     | 15.9  | 4.8         |
| 3       | 78          | 15.29   | 15.51 | 1.3         | 14.86     | 13.53 | 9.9         |
| 3       | 180         | 13.7  | 14.2  | 3.5         | 13.06     | 12.04 | 8.5         |
| 5       | 26          | 27.57   | 26.55 | 3.8         | 27.88     | 27.88 | 0           |
| 5       | 78          | 24.89   | 22.5  | 9.6         | 24.5      | 22.0  | 10.2        |
| 5       | 130         | 22.2  | 21.5  | 3.3         | 21.17     | 19.0  | 10.3        |

Theo., calculated value from the regression equations  
Exp., experimental value

of 112.5  $\mu\text{m}$ , sliding distance of 78 m). It may be noted further that the wear rate of the composite at the base level is higher than that of the matrix alloy. Thus it may be considered that the critical applied load (at which composite shows higher wear rate) for the composite is 4 N or less when the abrasive size is 112.5  $\mu\text{m}$ . The wear rate of these materials at random experimental conditions (within the selected experimental domain) is experimentally determined and compared with the calculated values using Eq (2) and (3) and are shown in Table 4. It clearly indicates that the experimental values are in close approximate (with maximum percent of deviation of 10.3) with the calculated values. This suggests the reliability of these empirical equations for predicting wear rates of the alloy and the composite within the selected experimental domain.

The above equations demonstrate that the effect of load and abrasive size is severe toward the wear rate of the materials (as coefficients associated with  $x_1$  and  $x_2$  are positive). However, between these two factors effect of load is more severe (coefficient associated with  $x_1$  is significantly higher). On the other hand, the wear rate of these materials reduces with increase in sliding distance (coefficient associated with  $x_3$  is negative). It may also be noted that interaction coefficient of load and abrasive size, and abrasive size, and sliding distance are positive, which signifies that the wear rate is further increased due to synergic effect of load and abrasive size or abrasive size and sliding distance. But the synergic effect of load and sliding distance reduces the wear rate of both the materials. Among these synergic effects of different parameters the synergic effect between load and abrasive size is significantly higher than the other ones. In general, the combined effect of all these factors (load, abrasive size, and sliding distance) is also causing more wear rate. However, this effect in the composite is negligible. If one compares the effect of each factor individually or their combined action on wear rate of each of the material, it may be noted that the effect of load is more or less same in the alloy and the composite. However, the effect of abrasive size is significantly higher in the composite. The effect of sliding distance is marginally higher in the composite as compared with the alloy. It may further be noted that the synergic effect of load and abrasive size is significantly higher in the composite than the matrix alloy. The synergic effect of load and sliding

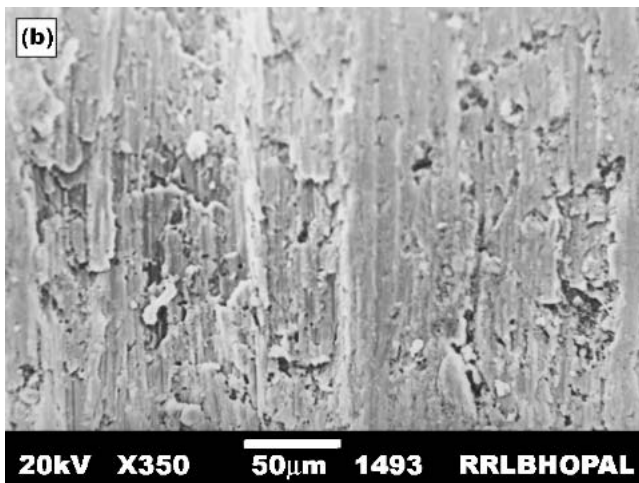
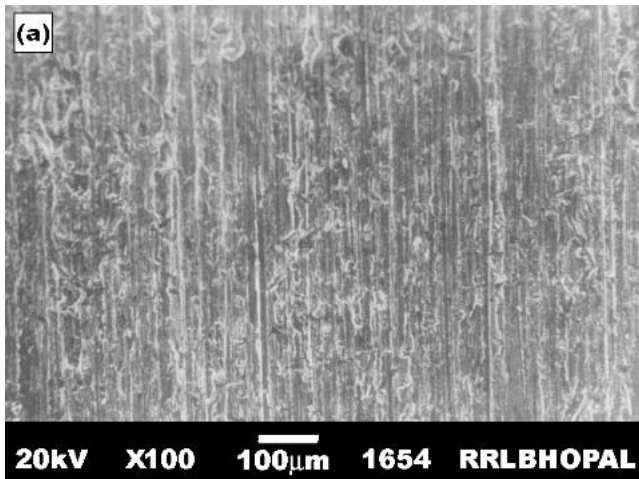


**Fig. 3** (a) Worn surface of the matrix alloy abraded against abrasives of size 25  $\mu\text{m}$  at an applied load of 1 N; (b) worn surface of the alloy abraded against abrasives of size 200  $\mu\text{m}$  at an applied load of 7 N

distance (towards reduction in wear rate) is also significantly higher in the composite.

On the other hand, synergic effect of abrasive size and sliding distance is considerably less in the composite unlike other two synergic effects. These equations also suggest that one must take into account the synergic effect of these experimental parameters in addition to their individual effects for predicting their wear rates.

### 3.3 Worn Surface

The worn surfaces of the selected samples were examined in SEM to understand the wear mechanism. Figure 3(a) represents the worn surface of the matrix alloy abraded against 25  $\mu\text{m}$  abrasive size at an applied load of 1 N. It clearly demonstrates continuous wear grooves and flakes along the wear tracks. This signifies that material is removed both by cutting and plowing actions. Figure 3(b) represents the worn surface of the alloy abraded against 200  $\mu\text{m}$  abrasive size at an applied load of 7 N. It is noted that the grooves are deeper and wider compared to that observed in Fig. 3(a). Figure 3(b) also shows large amount

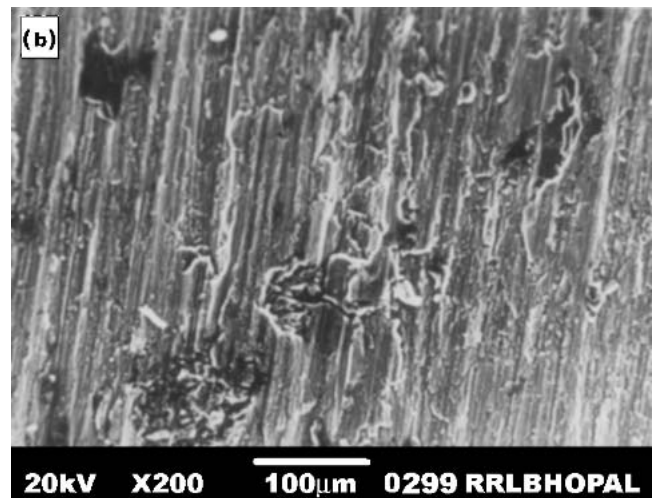
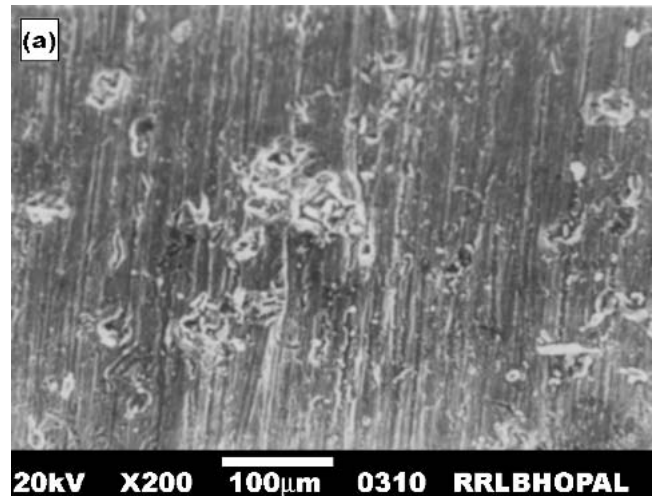


**Fig. 4** (a) Worn surface of the composite abraded against abrasives of size 25  $\mu\text{m}$  at an applied load of 1 N; (b) worn surface of the composite abraded against abrasives of size 200  $\mu\text{m}$  at an applied load of 7 N

of cavities due to removal of continuous flakes from the surface and large amount of surface cracks. It also demonstrates that in addition to cutting and plowing, tearing-type of material removal is taking place. Fig. 4(a) shows the worn surface of the composite abraded against the abrasive size of 25  $\mu\text{m}$  at an applied load of 1 N. It is noted that the wear grooves are continuous and much finer. The hard sillimanite particles are found to be present as protrusion on the worn surface. Figure 4(b) represents the worn surface of the composite when abraded against abrasive size of 200  $\mu\text{m}$  at an applied load of 7 N. It clearly indicates fracturing of sillimanite particles, which are removed from the worn surface and form cavities. It also represents tearing type of material removal as observed in Fig. 3(b).

## 4. Discussion

Abrasive particles in high-stress abrasion are fixed in their position as they are embedded on an emery paper cloth, which

in turn is rigidly fixed on a metallic wheel held against the specimens. Thus the abrasive particles cannot freely move, deflect, or change their position on the paper in which they are embedded. This results in transfer of total stress applied on the particles to the specimen surface. Under such condition abrasive particles penetrate into the specimen surface to the same depth irrespective of the nature of micro-constituents present in the material.<sup>[24]</sup> The depth of penetration is a function of factors such as stress level,<sup>[15,16]</sup> rake angles of the abrasive tip,<sup>[25]</sup> and hardness of the specimen surface subjected to wear. The penetration depth increases with increasing abrasive size, rake angles, and applied stress level, while it decreases with increasing the hardness of test materials. This leads to increase in wear rate with the increase in applied load and abrasive size. This is demonstrated by Eq (2) and (3) in which the coefficients associated with applied load ( $x_1$ ) and abrasive size ( $x_2$ ) are positive for both the materials.

The wear rate of the material is inversely proportional to the hardness. The composite is harder than the alloy due to the presence of hard sillimanite particles within the matrix. Hence it is expected that the composite should have a lower wear rate than that of the alloy. However, this may be possible so long the hard ceramic dispersoids remain intact within the matrix. The regression equations show that at the base level the composite (Eq 3) exhibits marginally higher wear rate than that of alloy (Eq 2). If the wear rate of the composite and alloy below the base level of the experimental parameters is calculated; it may be found that the composite exhibits a lower wear rate than that of the alloy at certain combination of load and abrasive size. This is also observed experimentally as shown in Table 4. Worn surfaces at 1 N load and 25  $\mu\text{m}$  abrasive size also indicate that depth and width of wear grooves are fine in case of the composite (Fig. 4a) as compared with that in the alloy (Fig. 3a), and the sillimanite particles are intact in the matrix which protect the soft matrix from wear (Fig. 4a). This fact clearly demonstrates that there is a critical load and abrasive size above which composite suffers from higher wear rate as compared with that of the alloy. The critical applied load and abrasive size are interrelated. If the abrasive size decreases, the critical applied load increases and vice versa. The critical applied load is 1 N when specimens are tested using the abrasive size of 200  $\mu\text{m}$  up to a sliding distance of 78 m. When the abrasive size is reduced to 112  $\mu\text{m}$ , the critical load is increased to 4 N. This may be attributed to the fact that different kinds of wear mechanisms are prevailing in the composite.

During two-body abrasion, a portion of load is applied on surface and subsurface deformation.<sup>[19]</sup> The hard ceramic dispersoids in the composite act as protrusion on the wear surface that bears the major portion of load and protect the matrix from destructive action of the abrasives (Fig. 4a). However, the applied loads are localized around these hard dispersoids.<sup>[26]</sup> When the localized stress around or over the ceramic dispersoids reach to a critical value, the sillimanite particles may not be able to withstand these stress levels, or the matrix may not be able to hold these ceramic particles within the surface. This leads to both fracture and fragmentation of ceramic particles, or scooping off of these particles (Fig. 4b) from the matrix.<sup>[24,27]</sup> Under these circumstances, the composite suffers from higher wear rate. The level of stress localization depends on applied load and abrasive size. It increases with increases in

both of these parameters. When abrasive size increases, the number of abrasive particles per unit area decreases. As a result, the applied load is shared by fewer abrasives and thus leads to higher effective stress level at the abrasive tips as well as on the specimen surface. In addition, the depth and width of the wear grooves increases with an increase in applied load and abrasive size, and if these are greater than the size of sillimanite particles, these particles could not offer any resistance against the abrasives. Thus, there is a greater possibility of removal of sillimanite particles (finer than abrasive particles) from the wear surface along with the cutting chips. As the matrix alloy in composite is plastically constrained, it is subjected to more surface cracking, which, in due course, reduces the capability of matrix alloy for holding the sillimanite particles in the worn surface (Fig. 4b). Further, the sillimanite particles (fragmented/scooped off) remain entrapped between the abrasive media and specimen surface and freely move over the wear surface. This generates three-body wear condition, in addition to two body and leads to more damage to the composite surface (Fig. 4b).

However, in the case of the alloy, the wear primarily takes place by cutting and plowing action and results in continuous wear grooves even at higher applied load and coarser abrasives. Additionally, under such conditions, there may be a possibility of temperature rise of the wear surface, which may cause the alloy softer. It facilitates spreading of flakes over the worn surface and finally some of the material is removed from the wear surface by tearing and/or delamination of flakes (Fig. 3b). Due to these facts, the coefficients associated with load ( $x_1$ ) and abrasive size ( $x_2$ ) have greater values in composites compared to those in the alloys. This also leads to significantly higher synergic effect of load and abrasive size ( $x_1x_2$ ) toward the wear of composite as compared with the alloy. However, it may be noted that the severity of the effect of abrasive size on the wear of composite is significantly higher with respect to its effect on the wear of the alloy whereas the severity of effect of load is marginally higher in composite. This may be due to the fact that even though load is increased, the abrasive size could not penetrate over a critical depth due to the limited size of abrasive. However, if abrasive size increases, even at lower applied load, it can penetrate more into the wear surface and cause great damage to the sillimanite particles due to increased stress level on individual coarser abrasive particles.

In the current study, a wear test was conducted using the same abrasive for the entire period. This led to the blunting, capping, shelling, and clogging of the abrasives.<sup>[28-31]</sup> All these facts reduced the destructive action of the abrasive media and hence reduced the rate of material removal. However, the blunting and shelling of abrasives may be more in case of composite due to the presence of hard sillimanite particles in it. As a result, it is expected that the rate of reduction in abrasive action of the abrasive medium may be higher when it moves over the composite surface. These facts lead to negative value of the coefficients associated with sliding distance ( $x_3$ ) and synergic effect of load and sliding distance ( $x_1x_3$ ). This also explains the higher value of these coefficients in composite as compared with that in the alloy.

It is, however, interesting to note that synergic effect of sliding distance and abrasive size is positive. It may be due to the fact that as abrasive size increases, stress level at the indi-

vidual abrasive tip increases and causes more damage to the material. Again, the inter-abrasive particle distance increases, which may not be able to accommodate fine debris within it and the abrasives, may be quite sharp for a long duration. As a result, the material is removed quite effectively and flakes are removed more frequently with increase in abrasive size and sliding distance (Fig. 3b and 4b). Thus, sliding distance does not annihilate the effect of the abrasive; rather it facilitates more material removal. But, the coefficient associated with synergic effect of abrasive size and sliding distance is less in the composite. This may be explained in line with the earlier discussion that the sillimanite particles cause great damage to the abrasive particles and the extent of such damage increases with increase in sliding distance and abrasive size.

In a nutshell, Eq (2) and (3) not only help to predict the wear rate of the composite and the alloy within the selected experimental domain, but is also quite useful in understanding the individual and synergic effect of the selected experimental parameters toward the wear of the materials. It clearly demonstrates the degree of severity of each factor, which was discussed earlier. A similar type of study can be conducted for understanding the effect of other experimental parameters like speed, microstructural characteristics like volume fraction of ceramic dispersoids, and mechanical properties of materials like strength, hardness, and toughness on the abrasive wear behavior of a material.

## 5. Conclusions

- 1) The effect of abrasive size on wear rate of the matrix alloy and the composite is severe but the effect of applied load is more severe. The wear rate of the materials decreases with increasing sliding distance. However, wear rate of the composite reduces more rapidly with sliding distance than with that observed in case of the alloy. The effect of load is more or less the same in the alloy and composite but the severity of the effect of abrasive size on wear of the composite is significantly higher than that in the alloy.
- 2) There is a critical applied load and abrasive size above which the composite shows high wear rate than that of alloy. The critical applied load and abrasive size are inter-related. The critical abrasive size decreases with increase in applied load and vice versa.
- 3) The synergic effect of applied load and abrasive size is significantly higher than the synergic effects due to other factors like abrasive size and sliding distance, and applied load and sliding distance.
- 4) Factorial design of experiments can be used successfully to develop empirical linear regression equations for predicting wear rate of the alloy and composite within a selected experimental domain. It also helps in understanding the severity of each factor as individual or in combination towards the wear of the alloy and composite.

## Acknowledgment

The authors are grateful to the Director of the Regional Research Laboratory in Bhopal for encouragement and permission to publish the results.

## References

1. A.I. Nussbaum: "New Application for Aluminium Based Metal Matrix Composites," *Light Metal Age*, 1997, pp. 54-58.
2. R. Chen, A. Iwabuchi, T. Shimizu, H.S. Stain, and H. Mifune: "The Sliding Wear Resistance Behaviour of NiAl and SiC Particles Reinforced Aluminium Alloy Matrix Composites," *Wear*, 1997, 213, pp. 175-84.
3. D.M. Schuster, M. Skibo, and F. Yep: "SiC Particles Reinforced Aluminium by Casting," *J. Metal*, 1987, 39, p. 60.
4. A.T. Alpas and J.D. Embury: "Sliding and Abrasive Wear Behaviour of an Aluminium (2014) SiC Particle Reinforced Composite," *Sci. Metall.*, 1990, 24, pp. 931-35.
5. A. Sato and R. Mehrabian: "Aluminium Matrix Composite Fabrication and Properties," *Metall. Trans.*, 1976, 7(B), pp. 443-51.
6. F.M. Hosking, F.F. Portillo, W. Wunderlin, and R. Mehrabian: "Composite of Aluminium Alloys," *J. Mater Sci*, 1982, 17, pp. 477-98.
7. K.J. Bhansali and R. Mehrabian: "Abrasive Wear of Aluminium-Matrix Composite," *J. Metall.* 1982, 34(9), pp. 30-34.
8. M.K. Surappa, S.V. Prasad, and R.K. Rohatgi: "Wear and Abrasion of Cast Al-Alumina Particle Composite," *Wear*, 1982, 77, pp. 295-302.
9. S.V. Prasad and P.K. Rohatgi: "Mechanism of Material Removal During Low Stress and High Stress Abrasion of Aluminium Alloy Zircon Particles Composite," *Mater. Sci. Eng.*, 1986, 80, pp. 213-20.
10. W.P. Caley, G.H. Kipouros, and P.W. Kingston: "The Potential Application of Natural Minerals Industries Minerals," *CIM Bulletin*, 1993, 86(968), pp. 116-21.
11. A.K. Jha, T.K. Dan, S.V. Prasad, and P.K. Rohatgi: "Alluminium Alloy-Solid Lubricant Talc Particle Composite," *J. Mater. Sci.*, 1986, 21, pp. 3681-85.
12. J. Yang and D.D.L. Chung: "Wear of Bauxite Particles-Reinforced Aluminium Alloys," *Wear*, 1989, 135, pp. 53-65.
13. K. Anand and Kishor: "On the Wear of Aluminium-Corundum Composite," *Wear*, 1983, 85, pp. 163-69.
14. M. Singh, O.P. Modi, R. Dasgupta, and A.K. Jha: "High Stress Abrasive Wear Behaviour of Aluminium Alloy Granite Particle Composite," *Wear*, 1999, 233-235, pp. 455-61.
15. D.P. Mondal, S. Das, A.K. Jha, and A.H. Yegneswaran: "Abrasive Wear of Al Alloy-Al<sub>2</sub>O<sub>3</sub> Particle Composite: A Study on the Combined Effect of Load and Size of Abrasive," *Wear*, 1998, 223, pp. 131-38.
16. S. Das, S. Gupta, D.P. Mondal, and B.K. Prasad: "Influence of Load and Abrasive Size on the Abrasive Wear of Al-SiC Composites," *Aluminium Trans.* 2000, 2(1), pp. 27-36.
17. L.J. Badse: "Influence of Grit Size on the Groove Formation During Sliding Abrasion," *Wear*, 1968, 11, p. 213.
18. E. Rabinowicz and A. Mutis: "Effect of Abrasive Particle Size on Wear," *Wear*, 1965, 18, p. 381.
19. M.A. Moore and R.M. Douthwaite: "Plastic Deformation Below Worn Surfaces," *Metall. Trans.*, 1976, 7A, pp. 1833-39.
20. A.T. Alpas and J.D. Embury: "Wear Mechanisms in Laminated and Particle Reinforced Metal Matrix Composites" in *Wear of Materials*, Vol. 1, K.C. Ludema and R.G. Bayer, ed. ASME, New York, NY, 1991, pp. 159-66.
21. S. Datta: "Application of Design of Experiment on Electrophoretic Deposition of Glass Ceramic Coating Materials From an Aqueous Bath," *Bull. Mater. Sci.*, 2000, 23(2), pp. 125-29.
22. R.J. Singh, S.N. Asthana, R. Ganguly, and B.K. Dhindaw: "Application of Design of Experiments to the Quantitative Study of the Strengthening Characteristics of Cast Al-Si-Mn-Mg Alloys," *Trans. Indian Inst. Met.*, 1989, 42, pp. 307-15.
23. P.K. Rohatgi, R. Asthana, and S. Das: "Solidification Structures and Properties of Cast Metal Ceramic Particle Composites," *Int. Met. Rev.*, 3(3), 1986, p. 115.
24. T. Kullik, T.H. Kosel, and Y. Xu: "Effect of Depth of Cut of Two Phase Alloys" in *Proc. Int. Conf. Wear Mater.* Vol. I, K.C. Ludema, ed., Denver, CO, 1989, pp. 23-33.
25. M.J. Murray, P.J. Mutton, and J.D. Watson: "Abrasive Wear Mechanisms in Steels," *J. Lubr. Technol., Trans. ASME Trib.*, 1982, 104, pp. 9-15.

26. R.L. Deuis, C. Subramanian, and J.M. Yellup: "Abrasive Wear of Aluminium Composites—A Review," *Wear*, 1996, 201, pp. 132-44.
27. B.K. Prasad, A.K. Jha, O.P. Modi, S. Das, and A.H. Yegneswaran: "Abrasive Wear Characteristics of Zn-37.2 Al-2.5 Cu-0.2 Mg Alloy Dispersed With Silicon Carbide Particles," *Mater. Trans. JIM*, 1995, 38, pp. 1048-57.
28. T.H. Kosel and N.F. Fiore: "Abrasive Wear in Multiphase Microstructures," *J. Mater. Energy Sys.*, 1981, 3, pp. 7-21.
29. A. Misra and I. Finnie: "On the Size Effect in Abrasive and Erosive Wear," *Wear*, 1980, 65, pp. 359-74.
30. T. Hisakado, H. Huda, and T. Trukui: "Effects of Dislodgment and Size of Abrasive Grains on Abrasive Wear," *Wear*, 1992, 155, pp. 297-307.
31. A.P. Mercer and I.M. Hutchings: "The Deterioration of Bonded Abrasive Papers During the Wear of Metals," *Wear*, 1989, 132, pp. 77-97.